

Background radiation from sterile neutrino decay and reionization

M. Mapelli & A. Ferrara

SISSA, Via Beirut 4, 34100, Trieste, Italy

13 August 2018

ABSTRACT

Sterile neutrinos are one of the most promising Warm Dark Matter candidates. By considering their radiative- and pion-decay channels, we derive the allowed contribution of sterile neutrinos to the X-ray, optical and near-infrared cosmic backgrounds. The X-ray background puts a strong constraint on the mass of radiatively decaying neutrinos ($m_{\nu_s} \lesssim 14$ keV), whereas the allowed mass range for pion-decay neutrinos (for a particle lifetime $> 4 \times 10^{17}$ s) is $150 \leq m_{\nu_s}/\text{MeV} \leq 500$. Taking into account these constraints, we find that sterile neutrinos do not significantly contribute to the optical and near-infrared background. We further consider the impact of sterile neutrinos on reionization. We find that the Thomson optical depth due to sterile neutrinos is $\tau_e = (0.4 - 3) \times 10^{-2}$ in the case of radiative decays, and it is $\approx 10^{-3}$ for the pion-decay channel. We conclude that these particles must have played only a minor role in cosmic reionization history.

Key words: neutrinos - cosmology: dark matter - infrared: general - X-rays: general

1 INTRODUCTION

Different dark matter candidates can be distinguished on the basis of their velocity dispersion, corresponding to a free-streaming length, below which dark matter fluctuations are suppressed. In Cold Dark Matter (CDM) models particles have negligible free-streaming length with respect to scales of cosmological interest. On the contrary, in Warm Dark Matter (WDM) scenarios the velocity dispersion of the particles is sufficient to smear out the fluctuations up to galactic scales, depending on the mass of the particles (Padmanabhan 1995). For this reason WDM models can alleviate the so called substructure crisis, which represents one of the most serious problems of CDM theories (Bode, Ostriker & Turok 2001; Ostriker & Steinhardt 2003).

Sterile neutrinos are considered the most promising WDM candidates (Colombi, Dodelson & Widrow 1996; Sommer-Larsen & Dolgov 2001). They can exist only if neutrinos have non-zero mass and mixing angles, as predicted by the standard oscillation theory (Dolgov & Hansen 2002; see Dolgov 2002 for a complete review of sterile neutrino properties). They are massive; so they can decay into lighter particles, following a large number of different possible channels (Dolgov 2002). Among all the possible decay processes, those which lead to the emission of photons are particularly interesting, because we can put constraints on the existence, the mass, the lifetime, and other properties of sterile neutrinos, depending on the detection of such radi-

ation (De Rújula & Glashow 1980; Stecker 1980; Drees & Wright 2000; Abazajian, Fuller & Patel 2001a; Abazajian, Fuller & Tucker 2001b; Dolgov 2002 and reference therein). In principle, radiation due to neutrino decays should be seen both as line emission in the local universe (at energy $E_\gamma = (m_{\nu_s}^2 - m_{\nu_a}^2)/2m_{\nu_s}$, where m_{ν_s} and m_{ν_a} are respectively the mass of the sterile and of the light neutrino), and as background radiation, given by the integrated contribution of decays occurring at different redshifts. Until now, none of the experiments built to detect emission lines in the local universe has provided any evidence of the existence of sterile neutrinos (Henry & Feldman 1981; Shipman & Cowsik 1981; Holdberg & Barger 1985; Bowyer et al. 1999). The absence of detection can be used to fix upper limits on the mass and lifetime of sterile neutrinos. In particular, measurements of X-ray emission from galaxy clusters (Abazajian, Fuller & Tucker 2001b) provide a strong upper limit of the rest mass of radiatively decaying sterile neutrinos ($m_{\nu_s} \lesssim 5$ keV in the zero lepton production mode). This limit is particularly constraining, given that studies (based on Ly α forest data) of power spectrum fluctuations due to free-streaming effects provide a lower limit for the mass of sterile neutrinos $m_{\nu_s} \gtrsim 2$ keV (Viel et al. 2005; see also Narayanan et al. 2000¹). Studies of cosmological contributions of sterile neutrinos to the background radiation in

¹ The lower limit of 0.75 keV for thermal neutrino mass derived by Narayanan et al. (2000) can be converted into a lower limit

different bands (Stecker 1980; Kimble, Bowyer & Jakobsen 1981; Ressel & Turner 1990; Davidsen et al. 1991; Abazajian, Fuller & Tucker 2001b) can only provide upper limits of their mass and lifetime. In addition, upper limits derived from background radiation can be biased by dark matter clustering (Abazajian, Fuller & Tucker 2001b).

It has also been proposed that radiatively decaying sterile neutrinos can be responsible of the reionization (Sciama 1982; Rephaeli & Szalay 1981; Sciama 1990; Sciama 1993). This idea does not encounter particular success today, because there are no observational evidences supporting it. The main failure of this model is that the ionizing sources proposed by Sciama, sterile neutrinos of mass $m_{\nu_s} = 27.4 \pm 0.2$ eV, must be excluded on the basis of the lower limit derived by the power spectrum analysis (Narayanan et al. 2000; Viel et al. 2005). On the other hand, even if it seems unlikely that sterile neutrinos are the only responsible of the reionization, we cannot exclude that they partially contribute to it, together with other sources. Furthermore, the high electron scattering optical depth ($\tau_e = 0.17 \pm 0.04$) resulting by WMAP data (Spergel et al 2003; Kogut et al. 2003), combined with the indication that the universe was not fully ionized until redshift 6-7, as one can derive from the HI absorption present in the spectra of highest redshift quasars in the Sloan Digital Sky Survey (Becker et al. 2001; Fan et al. 2003), suggests a long (and, maybe, complex) reionization history, difficult to achieve considering only "traditional sources" (as Population II stars and quasars). One of the proposed scenarios (Cen 2003; Furlanetto & Loeb 2004) predicts a first high redshift phase of partial ionization, triggered by quite exotic objects, followed by a most recent phase of complete and definitive re-ionization, ended at redshift about 6 and due to normal Population II stars and quasars. Among the various candidates proposed as sources of the first partial ionization, like massive metal-free stars (Haiman & Holder 2003; Choudhury & Ferrara 2004) and micro-quasars (Madau et al. 2004), one could reasonably include also radiatively decaying neutrinos.

As an alternative, Hansen & Haiman (2004, hereafter HH) have recently suggested that also sterile neutrinos which do not directly decay into photons can be a source of this partial ionization. They noticed that very massive sterile neutrinos ($140 \leq m_{\nu_s} \leq 500$ MeV) mainly decay into pions and leptons (electrons or positrons). These electrons are sufficiently energetic to Compton-scatter CMB photons, which can then ionize hydrogen atoms directly or through secondary electrons.

In this paper we want to check the possible contribution of sterile neutrinos to the background radiation, in the light of the most recent measurements of the extragalactic background light (EBL), with particular care for the optical-infrared (Madau & Pozzetti 2000; Bernstein et al. 2002; Matsumoto et al. 2000; Wright 2000) and for the X-ray band (Gruber 1992; Hornschmeier et al. 2001; Tozzi et al. 2001; Moretti et al. 2003 [M03]; Dijkstra et al. 2004 [D04]; Bauer et al. 2004 [B04]). We, further, discuss the role of radiatively and pion-decaying sterile neutrinos in the cosmic

reionization, calculating the corresponding Thomson optical depth.

2 LIGHT FROM NEUTRINO DECAYS

In this Section we calculate the possible contribution of sterile neutrinos decaying at different redshifts to the observed background flux.

2.1 Radiative decay channel

To start, let us consider the case of radiatively decaying neutrinos. Radiative decay is one of the possible outcomes of the following process.

$$\nu_s \rightarrow \nu_a + l + l, \quad (1)$$

where ν_s is the sterile neutrino, ν_a is an ordinary active neutrino and l is a lepton. In particular, this decay is radiative when the two leptons in the previous expression are an electron-positron pair, their annihilation producing a photon. This photon has an energy $E_\gamma = (m_{\nu_s}^2 - m_{\nu_a}^2)/2m_{\nu_s}$. Stecker (1980) calculated the flux emitted by sterile neutrinos radiatively decaying at different redshift. Correcting its calculations and updating them to present values of cosmological parameters², we find a photon flux (units of $\text{cm}^{-2} \text{s}^{-1} \text{sr}^{-1}$):

$$I(E_{obs}) = \frac{n_s c}{4\pi H_0 \tau} \int_0^z \frac{e^{-t(z)/\tau} E_0 \delta((1+z)E_{obs} - E_0)}{(1+z) [(1+z)^3 \Omega_{0M} + \Omega_\Lambda]^{1/2}} dz, \quad (2)$$

where n_s and τ are the present number density and the lifetime of sterile neutrinos respectively; E_0 and E_{obs} are the emitted and the observed energy of the photon, and $t(z)$ is the time elapsed from the Big Bang to redshift z , which can be approximated at high redshift as

$$t(z) \simeq \frac{2}{3} H_0^{-1} \Omega_{0M}^{-1/2} (1+z)^{-3/2} \quad (3)$$

Since $\delta((1+z)E_{obs} - E_0) \neq 0$ if and only if $(1+z) = E_0/E_{obs}$, the eq. (2) becomes (for comparison, see Massó & Toldrà 1999)

$$I(E_{obs}) = \frac{1}{4\pi} \frac{c}{H_0} \frac{n_s}{\tau} \frac{e^{-t(E_0/E_{obs})/\tau}}{[(E_0/E_{obs})^3 \Omega_{0M} + \Omega_\Lambda]^{1/2}} \quad (4)$$

This equation depends on two fundamental, substantially unknown, parameters: the density n_s and the lifetime τ of sterile neutrinos. A reasonable upper limit of n_s can be obtained by imposing that all the dark matter is composed by sterile neutrinos (Dolgov & Hansen 2002):

$$\frac{n_s}{n_a} = 1.2 \times 10^{-2} \left(\frac{\text{keV}}{m_{\nu_s}} \right) \left(\frac{\Omega_{DM}}{0.23} \right) \left(\frac{h}{0.72} \right)^2, \quad (5)$$

where n_a is the present density of active neutrinos and m_{ν_s} is the mass of sterile neutrinos.

The lifetime τ can be expressed as a function of n_s and m_{ν_s} , as follows. The rate Γ for the process (1) is given by

² We adopt the following cosmological parameters: Hubble constant $H_0=72 \text{ km s}^{-1} \text{ Mpc}^{-1}$, $\Omega_{0M} \equiv \Omega_{DM} + \Omega_b=0.27$, $\Omega_\Lambda=0.73$, which are in agreement with the recent WMAP determination (Spergel et al. 2003).

of ~ 2 keV for sterile neutrino mass, as shown by Hansen et al. (2002).

(Boehm & Vogel 1987; Drees & Wright 2000; Abazajian, Fuller & Patel 2001a):

$$\Gamma = \frac{\sin^2(2\theta)}{768\pi^3} G_F^2 m_{\nu_s}^5 \simeq \frac{\sin^2\theta}{192\pi^3} G_F^2 m_{\nu_s}^5, \quad (6)$$

where θ is the mixing angle and G_F the Fermi constant. The branching ratio for radiative decay, that is the fraction of processes of type (1) leading to the emission of a photon, can be expressed as (Drees & Wright 2000):

$$B = \frac{27\alpha_{em}}{8\pi} \quad (7)$$

where α_{em} is the fine structure constant. Then, the rate $\Gamma_{rad} \equiv \tau^{-1}$ of radiative neutrino decays is the following.

$$\Gamma_{rad} = \frac{9\alpha_{em}}{512\pi^4} \sin^2\theta G_F^2 m_{\nu_s}^5, \quad (8)$$

where $\sin^2\theta$ can be written as (Dolgov & Hansen 2002³):

$$\sin^2\theta = 2.8 \times 10^{-6} \frac{n_s}{n_a} \frac{c_2^{1/2}}{(1+g_L^2+g_R^2)} \left(\frac{\text{keV}}{m_{\nu_s}}\right) \left(\frac{g}{10.75}\right)^{3/2}, \quad (9)$$

where c_2 is a numerical coefficient depending on the neutrino flavor ($c_2 = 0.61$ for ν_e and $c_2 = 0.17$ for ν_τ and ν_μ) and g is the number of relativistic degrees of freedom at the time when sterile neutrinos were produced (we adopted $g = 10.75$, Viel et al. 2005); finally, $g_R \equiv \sin^2\theta_W$ and $g_L \equiv 1/2 + \sin^2\theta_W$, where $\sin^2\theta_W = 0.23$ (Dolgov & Fukugita 1992), θ_W being the weak mixing angle.

2.2 Pion decay channel

We can derive the same quantities calculated for radiative decays in the case of pion decay considered by HH. They noticed that, if the sterile neutrino has a mass in the range 140-500 MeV, the dominant decay channel is (Astier et al. 2001)

$$\nu_s \rightarrow l + \pi, \quad (10)$$

where π is a pion and l can be an electron, a positron or a neutrino. We will focus on the case in which l is an electron. It will have an energy $E_e = (m_{\nu_s} - m_\pi)/2$, where m_π is the pion total mass. Then, because the rest mass of the pion is 139.7 MeV, $0 < E_e < 180$ MeV. As pointed out by HH, an electron in this range of energies has a mean free path to inverse Compton-scattering with CMB photons generally lower than the mean free path to collisionally ionizing hydrogen. Then the most important interaction these electrons will experience is the inverse Compton-scattering with CMB photons. Can these scattered CMB photons significantly contribute to the background radiation? To answer this question we made the following calculations. As a first approximation, we assume that the electrons produced by neutrino decay follow a power law energy distribution with spectral index p (this assumption takes into account the fact that each electron interacts more than once with CMB photons, gradually degrading its energy). The final spectrum

of photons, initially a Planckian, due to inverse Compton-scattering by a power law distribution of electrons is given by (Abramowitz & Stegun 1965; Rybicki & Lightman 1979)

$$\frac{dE}{dV dt dE d\Omega} = \frac{1}{4\pi} \frac{8\pi^2 r_0^2 A}{h_{Pl}^3 c^2} F(p) (k_B T)^{(p+5)/2} E^{-(p-1)/2} \quad (11)$$

where r_0 is the classical radius of the electron, h_{Pl} the Planck constant, k_B the Boltzmann constant, T the initial black body temperature of photons, p the spectral index of the electron distribution and E the final photon energy. $F(p)$ is defined by:

$$F(p) = 2^{(p+3)} \frac{p^2 + 4p + 11}{(p+3)^2(p+5)(p+1)} \Gamma\left(\frac{p+5}{2}\right) \zeta\left(\frac{p+5}{2}\right),$$

where Γ is the Euler's Gamma function and ζ is the Riemann's Zeta function. A is a normalization factor defined by

$$n_e = \int_{\gamma_{min}}^{\gamma_{max}} A \gamma^{-p} d\gamma \quad (12)$$

where n_e and γ are respectively the density and the Lorentz factor of the electrons ($0 < \gamma < 360$).

We included in eq. (11) the dependences on the redshift and we integrated it over the line-of-sight, obtaining the following equation.

$$\begin{aligned} I(E_{obs}) &= \int_0^z \frac{dE}{dV dt dE d\Omega} \frac{dl}{dz} dz \\ &= \frac{1}{4\pi} \frac{8\pi^2 r_0^2}{h_{Pl}^3 c^2} F(p) (k_B T_0)^{(p+5)/2} E_{obs}^{-(p-1)/2} \\ &\quad \times \frac{c}{H_0} \int_0^z \frac{A(z)(1+z)^{-1}}{[(1+z)^3 \Omega_{0M} + \Omega_\Lambda]^{1/2}} dz \end{aligned} \quad (13)$$

where T_0 is the present temperature of the CMB⁴ and $E_{obs} \equiv E(1+z)$ is the final energy of the photon at redshift $z=0$. $A(z)$ can be derived from eq. (12). In particular we want to express the proper density of electrons $n_e(z)$ as a function of the initial density of sterile neutrinos $n_s(z)$ and of their lifetime τ . The production rate of electrons is approximately given by $dn_e/dt = n_s(z) \exp[-t(z)/\tau]/\tau$. Integrating, we obtain

$$n_e(t) = \int_0^t \frac{n_s(z)}{\tau} e^{-\tilde{t}(z)/\tau} f(\tilde{t}) d\tilde{t} \quad (14)$$

where $f(t)$ is a function which takes into account the fact that the electrons have a finite lifetime. In the simplest case, $f(t)$ is a step function

$$f(\tilde{t}) = \begin{cases} 1 & \text{if } (t(z) - t_C(z)) < \tilde{t} < t(z) \\ 0 & \text{otherwise} \end{cases}$$

where $t_C(z)$ is defined as the electron cooling time due to repeated Compton-scatterings with CMB photons, $t_C(z) \sim 6 \times 10^4 (E_e/100 \text{ MeV})^{-1} [(1+z)/21]^{-4}$ yr (HH). Substituting $f(t)$ in eq. (14), we obtain:

$$\begin{aligned} n_e(t) &= \int_{(t(z)-t_C(z))}^{t(z)} \frac{n_s(z)}{\tau} e^{-\tilde{t}(z)/\tau} d\tilde{t} \\ &= n_s(z) e^{-t(z)/\tau} (e^{t_C(z)/\tau} - 1) \end{aligned} \quad (15)$$

³ In equation (12) of Dolgov & Hansen 2002 the term $\left(\frac{g}{10.75}\right)^{-1/2}$ should be $\left(\frac{g}{10.75}\right)^{3/2}$ (S. Hansen private communication).

⁴ We adopted $T_0 = 2.275$ K (Spergel et al. 2003).

where $t(z)$ is computed according to eq. (3).

Finally $n_s(z) = n_s(1+z)^3$ (where n_s is the present sterile neutrino density) can be easily expressed as a function of the present density of active neutrinos n_a and of the lifetime τ and the mass $m_{\nu s}$ of sterile neutrinos (HH):

$$n_s \sim \frac{4.8}{(m_{\nu s}/m_\pi)^2 - 1} n_a \tau^{-1} \quad (16)$$

Taking into account that $n_a = \frac{3}{11} n_b/\eta$ (where n_b is the present baryon density and η is the present baryon-to-photon ratio⁵), we finally obtain:

$$A(z) = \frac{4.8(1+z)^3}{[(m_{\nu s}/m_\pi)^2 - 1]} \frac{3n_b}{11\eta} \frac{\tau^{-1}}{\int_{\gamma_{min}}^{\gamma_{max}} \gamma^{-p} d\gamma} \times e^{-t(z)/\tau} (e^{t_C(z)/\tau} - 1), \quad (17)$$

which can be substituted into eq. (13).

3 BACKGROUND RADIATION

Now we have all the equations we need to estimate the contribution of sterile neutrinos to the background radiation. Using eqs. (4) and (13) we can derive the observed flux respectively due to radiative and not-radiative neutrino decays. In our calculations, we assume that all the photons produced (or Compton-scattered) by neutrinos decaying at $z > 1000$ are thermalized by CMB photons, and then are not visible. We assume also, for simplification, that all the photons produced (or Compton-scattered) by neutrinos decaying at $z < 1000$ are not absorbed or scattered. For this reason, our calculation represents an upper limit for the optical and infrared background; however it should give a good estimate of the X-ray flux.

3.1 Soft X-ray background

A recent estimate of the soft X-ray background (SXRb), in the energy range 0.5-2.0 keV, is provided by M03. Combining 10 different measurements reported in the literature, they found a flux of $2.47 \pm 0.11 \times 10^{-8} \text{ erg s}^{-1} \text{ cm}^{-2} \text{ sr}^{-1}$, which must be lowered to about $1.48 \times 10^{-9} \text{ erg s}^{-1} \text{ cm}^{-2} \text{ sr}^{-1}$, if the mean contribution of both point and diffuse unresolved sources is subtracted at the level estimated by M03. D04 derive the slightly lower value $1.15 \pm 1.64 \times 10^{-9} \text{ erg s}^{-1} \text{ cm}^{-2} \text{ sr}^{-1}$, as they subtract a further 1.0-1.7% contribution by the diffuse component due to Thomson-scattered point source radiation (Soltan 2003). D04 also suggest a maximum possible value $\sim 4.04 \times 10^{-9} \text{ erg s}^{-1} \text{ cm}^{-2} \text{ sr}^{-1}$, by subtracting the lower limit of unresolved sources and of Thomson scattered flux. D04 further notice that the theoretically expected amount of X-ray emission in the soft band from thermal emission by gas in clusters (Wu & Xue 2001) should represent $\sim 9\%$ of the total SXRb, considerably higher than the 6% estimated by M03. However, D04 do not include in their estimate of the background this probable additional contribution. Otherwise, the flux due to unaccounted sources should be lowered to $\sim 4.0 \times 10^{-10} \text{ erg s}^{-1} \text{ cm}^{-2} \text{ sr}^{-1}$.

⁵ We used $n_b = 2.7 \times 10^{-7} \text{ cm}^{-3}$ and $\eta = 6 \times 10^{-10}$, according to WMAP (Spergel et al. 2003).

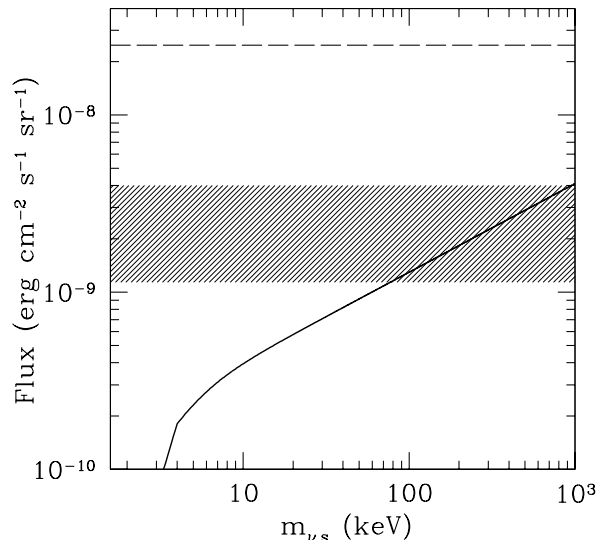


Figure 1. Integrated flux between 0.5 and 2 keV due to radiatively decaying neutrinos as a function of the neutrino mass (*solid line*). The horizontal *dashed line* represents the total measured background (M03). The shaded area indicates the flux due to unresolved sources (B04).

More recently, B04 investigated the X-ray number counts in the Chandra Deep Fields (CDFs). Adopting for the total SXRb from 0.5 to 2 keV the value suggested by M03 (i.e. $2.47 \pm 0.11 \times 10^{-8} \text{ erg s}^{-1} \text{ cm}^{-2} \text{ sr}^{-1}$), they found that its resolved fraction is $89.5^{+5.9}_{-5.7}\%$. The resolved sources are predominantly AGNs ($\sim 83\%$) and star forming galaxies ($\sim 3\%$). This means that unresolved sources produce a flux $2.59^{+1.41}_{-1.46} \times 10^{-9} \text{ erg s}^{-1} \text{ cm}^{-2} \text{ sr}^{-1}$.

These strong limits on the SXRb are important to constraint the mass of sterile neutrinos. We base our analysis on the paper by B04; in addition we have checked the values derived by M03 and by D04. The latter are consistent with those reported by B04 and give only slightly different constraints on the sterile neutrino mass. In Fig. 1 we report the integrated flux between 0.5 and 2 keV due to radiative neutrino decays for different neutrino masses. To calculate this flux we derived the neutrino comoving density from eq. (5), i.e. assuming that all the dark matter is due to sterile neutrinos. Given the mass and the density, the lifetime is completely determined by eqs. (8) and (9). The flux due to sterile neutrinos is compared with the total flux predicted by M03 and with the flux due to unresolved sources (B04). As we can see from Fig. 1, only neutrinos with masses $\lesssim 950$ keV do not exceed the maximum value of the flux due to unresolved sources ($4.00 \times 10^{-9} \text{ erg s}^{-1} \text{ cm}^{-2} \text{ sr}^{-1}$, B04); the same conclusion can be drawn by using D04 data.

We repeat the same calculation for heavy sterile neutrinos ($140 < m_{\nu s} < 500 \text{ MeV}$) decaying into pions and electrons. In this case we consider the flux due to CMB photons Compton-scattered by the electrons coming from the neutrino decay (eq. (13), assuming $p=1$). Fig. 2 shows the isocontours of the integrated flux between 0.5 and 2 keV due to Compton-scattered CMB photons, as a function of the progenitor neutrino mass and lifetime. As we can see

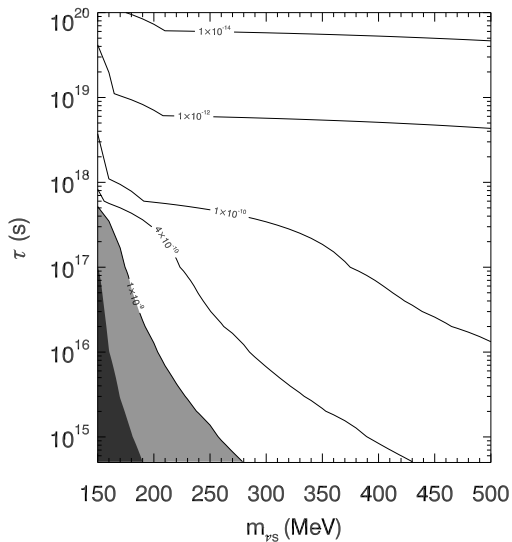


Figure 2. Isocontours of integrated X-ray flux in the band 0.5-2 keV (units of $\text{erg cm}^{-2} \text{s}^{-1} \text{sr}^{-1}$) due to pion-decaying neutrinos as a function of the neutrino mass and lifetime. The light gray area indicates flux due to unresolved sources (B04). The dark gray area indicates the "forbidden" region in which the flux exceeds the maximum background flux due to unaccounted sources (B04; M03).

from the eq. (16), the density of neutrinos depends strongly on their mass and on the lifetime. In particular, less massive neutrinos have much higher comoving density. For this reason, and because of the largely different mass range, the observed flux has an opposite behavior with respect to radiatively decaying neutrinos. In this case the soft X-ray flux decreases increasing the neutrino mass. The flux produced by 150-500 MeV neutrinos does not violate the SXR limit (B04), if the lifetime is $\geq 10^{17}$ s. For shorter lifetimes, neutrinos with mass lower than 190 MeV do violate the constraint imposed by unresolved sources, according to both M03/D04 and B04 estimates.

3.2 Hard X-ray background

M03 estimated the total background flux in the hard band (2-10 keV, HXRB) to be $6.63 \pm 0.36 \times 10^{-8} \text{ erg cm}^{-2} \text{ s}^{-1} \text{ sr}^{-1}$. They also show that the resolved fraction of this background is $88.8_{-6.6}^{+7.8}\%$. Then only the 11.2% of the hard X-ray background can be due to unaccounted sources (like sterile neutrinos).

B04 studied the HXRB flux from 2 to 8 keV, using the X-ray number counts in the CDFs. They adopted a total HXRB flux $5.88 \pm 0.36 \times 10^{-8} \text{ erg cm}^{-2} \text{ s}^{-1} \text{ sr}^{-1}$ and found that the resolved fraction is $92.6_{-6.3}^{+6.6}\%$, dominated by AGNs ($\sim 95\%$). This means that the unresolved flux is only $4.35_{-3.88}^{+3.70} \times 10^{-9} \text{ erg cm}^{-2} \text{ s}^{-1} \text{ sr}^{-1}$.

We compared the hard X-ray flux due to sterile neutrinos with the background level estimated by B04, and we checked for consistency with M03. In particular, for radiatively decaying sterile neutrinos we found that the integrated flux in the range 2-8 keV is lower than the background

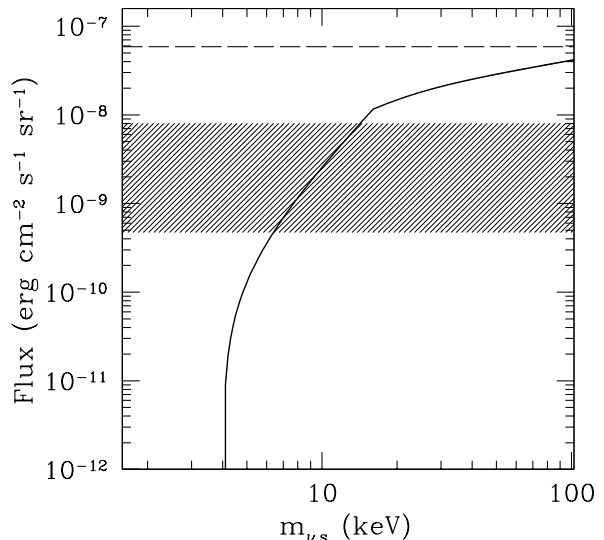


Figure 3. Integrated X-ray flux in the range 2-8 keV due to radiatively decaying neutrinos as a function of the neutrino mass (solid line). The horizontal dashed line indicates the total background in the same band; the shaded area indicates the flux due to unresolved sources (B04).

flux due to unresolved sources, as estimated by B04, only if $m_{\nu_s} \lesssim 14$ keV (Fig. 3). If we consider the unresolved flux in the range 2-10 keV estimated by M03, we find a similar constraint for the neutrino mass: $m_{\nu_s} \lesssim 16$ keV. This is a strong constraint, if combined with the lower limit for the sterile neutrino mass $\gtrsim 2$ keV derived by Viel et al. 2005. We must be aware of two uncertainties in our calculations. First, we made the assumption that all the dark matter is composed by sterile neutrinos. In addition, we have not taken into account the clustering of matter at low redshift, which can lead to an overestimate of the flux due to neutrinos (Abazajian et al. 2001b).

On the other hand, the integrated flux (in the range 2-8 keV) of CMB photons scattered by heavy pion-decay neutrinos is lower than the upper limit of the background due to unresolved sources (B04) for all the neutrino masses from 150 to 500 MeV, if the lifetime is longer than $\sim 4 \times 10^{17}$ s (Fig. 4). We obtain the same result by considering (in the range 2-10 keV) the flux due to unaccounted sources as estimated by M03. For shorter lifetimes, the minimum allowed mass increases. For example, if $\tau = 10^{15}$ s, neutrinos with masses lower than ~ 215 MeV exceed the upper limit of the background due to unresolved sources as derived by B04; whereas, using the estimate of M03, we find ~ 200 MeV.

In summary, using the HXRB we put much stronger constraints on the mass of radiatively decaying neutrinos ($m_{\nu_s} \lesssim 14$ keV) than using the SXR. Instead, in the case of heavy sterile neutrinos decaying into pions, all the masses from 150 to 500 MeV are allowed, provided a lifetime longer than 4×10^{17} s.

To compare our results with those obtained by Abazajian et al. (2001b), we have repeated this analysis using Gruber's model of HXRB (1992). We found that, assuming this

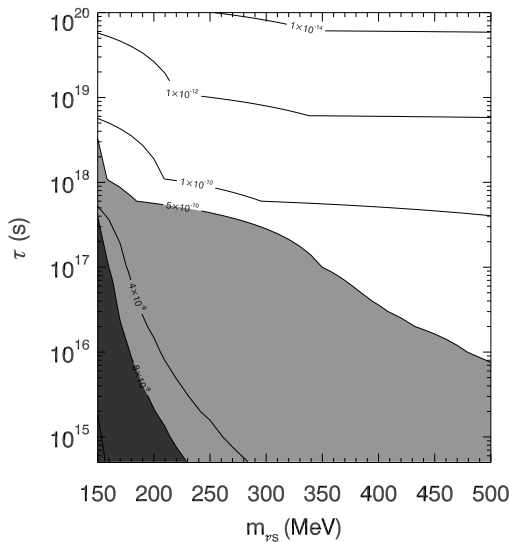


Figure 4. Isocontours of the integrated X-ray flux in the band 2-8 keV (units of $\text{erg cm}^{-2} \text{s}^{-1} \text{sr}^{-1}$) due to pion-decaying neutrinos as a function of the neutrino mass and lifetime. The light gray area indicates the flux due to unresolved sources (B04). The dark gray area indicates the "forbidden" in which the flux exceeds the maximum background flux due to unresolved sources (B04).

model of HXRB, the mass of radiatively decaying neutrinos must be $m_{\nu s} \lesssim 3$ keV, in agreement with Abazajian et al. (2001b). However, in the following we will use the constraints derived using the estimates by B04 and M03, because they come from more recent data and do not require any assumption about the shape of the HXRB due to unresolved sources.

3.3 Optical and near-infrared (NIR) background

A number of factors, such as interplanetary dust scattered sunlight (zodiacal light), terrestrial airglow, dust-scattered Galactic starlight (diffuse Galactic light), make very difficult to obtain a reliable measurement of the NIR and especially of the optical background light. Here we briefly summarize the most recent measurements of optical and NIR background. Deep optical and NIR galaxy counts give an estimate of the EBL fraction coming from normal galaxies. Madau & Pozzetti (2000) derived the contribution of known galaxies in the *UBVIJHK* bands from the *Southern Hubble Deep Field* imaging survey. In particular for the U, V, B and I bands (corresponding to the wavelengths $\lambda = 3600, 4500, 6700$ and 8100 \AA) they found a mean flux respectively $2.87^{+0.58}_{-0.42}$, $4.57^{+0.73}_{-0.47}$, $6.74^{+1.25}_{-0.94}$ and $8.04^{+1.62}_{-0.92}$ in units of $10^{-6} \text{ erg s}^{-1} \text{ cm}^{-2} \text{ sr}^{-1}$. Following a different approach, Bernstein et al. (2002) measured the mean flux of the optical EBL at 3000, 5500, and 8000 \AA , using the Wide Field Planetary Camera 2 (WFPC2) and the Faint Object Spectrograph, both on board the *Hubble Space Telescope*, combined with the du Pont 2.5 m Telescope at the Las Campanas Observatory. They found for these three band a mean flux of the EBL respectively $12.0^{+17.7}_{-6.3}$, $14.9^{+19.3}_{-10.5}$, and

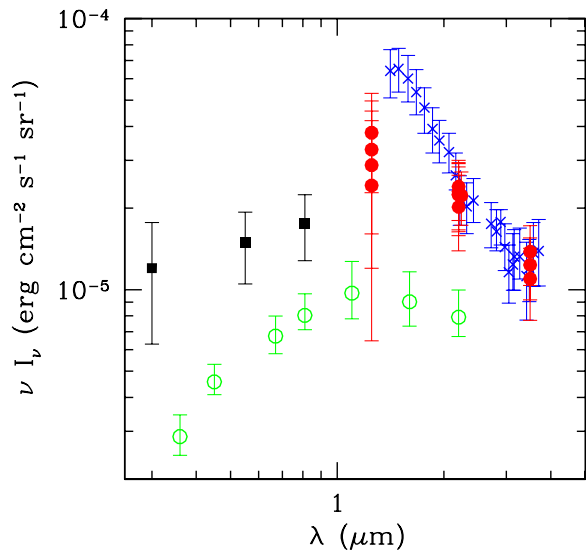


Figure 5. Measurements of the optical and NIR background: Bernstein et al. (*filled squares*); Madau & Pozzetti (*open circles*); Matsumoto et al. (*crosses*); DIRBE data reduced adopting the Wright model of zodiacal light (*filled circles*).

$17.6^{+22.4}_{-12.8}$ in units of $10^{-6} \text{ erg s}^{-1} \text{ cm}^{-2} \text{ sr}^{-1}$, considerably higher than the contribution of the galaxy counts alone.

The available NIR background data come from the Diffuse Infrared Background Experiment (DIRBE) on board of the Cosmic Background Explorer (COBE) and from the Near InfraRed Spectrometer (NIRS) on board of the InfraRed Telescope in Space (IRTS). A summary of the DIRBE results can be found in Hauser et al. (1998). Matsumoto et al. (2000) made a preliminary analysis of the NIRS data, estimating the NIRB on the basis of the 5 NIRS observation days unperturbed by atmospheric, lunar and nuclear radiation effects. Both the DIRBE and the NIRS data show an excess in the NIRB with respect to galaxy counts. The amount of this excess depends on the model used to subtract the contribution of the zodiacal light from the measurements. In fact, there are two different models of zodiacal light, that described in Kelsall et al. (1998) and that presented by Wright 1997 (see also Wright 1998 and Wright & Reese 2000). Fig. 5 presents a summary of all the data we have considered.

The measurements of the NIR and, with less evidence, of the optical background, seem to indicate the presence of an excess with respect to galaxy counts. The most plausible explanation of the NIR excess is that the extragalactic background light in this wavelength range is due to the redshifted UV and optical light emitted by Pop III stars (Bond, Carr & Hogan 1986; Santos, Bromm & Kamionkowski 2002; Salvaterra & Ferrara 2003). In particular Salvaterra & Ferrara (2003) developed a model of the NIR background which, accounting for the most recent predictions of Pop III stellar spectra (Schaefer 2002) and IMF, nebular emission (i.e. the radiation coming from the nebula surrounding the star), and $L_{\gamma\alpha}$ photons scattered by the intergalactic medium, is able to fit the NIRS data (Matsumoto et al. 2000) and the

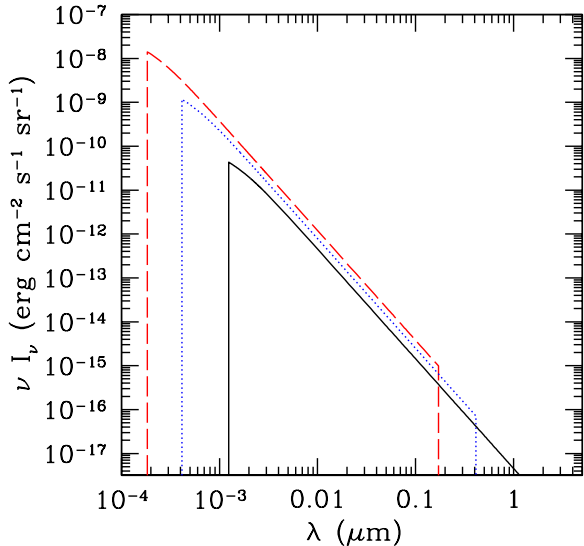


Figure 6. Background due to radiatively decaying neutrinos with mass 14 keV (*dashed line*), 6 keV (*dotted*) and 2 keV (*solid*).

DIRBE data with both the methods of zodiacal light subtraction. This model is supported also by the analysis of the infrared background fluctuations performed by Magliocchetti et al. (2003).

In principle, sterile neutrinos could be an additional source of optical and infrared light (Stecker 1980; Biller et al. 1998). In this Section we want to check this hypothesis, calculating the contribution of sterile neutrinos (in the range of masses and/or lifetimes allowed by the constraints derived from the HXRFB) to the optical and infrared background and comparing it with observational data.

In Fig. 6 we plot the contribution to the background light by radiatively decaying neutrinos for three different allowed masses (respectively 2, 6 and 14 keV). We derived their density by assuming that all the dark matter is composed by sterile neutrinos. The lifetime is uniquely determined by the neutrino density and mass. We conclude that the flux due to radiatively decaying neutrinos in the optical and infrared background is completely negligible, being at least 8 order of magnitudes lower than the observational data (shown in Fig. 5) even in the most favorable hypothesis. We notice that the cut-off at low energy is due to the assumption that photons emitted at $z > 1000$ are completely thermalized. The high energy cutoff simply follows from the fact that it has to be $z \geq 0$.

Fig. 7 shows that also the optical and infrared background due to CMB photons Compton-scattered by electrons which are the product of the decay of massive sterile neutrinos⁶ is negligible with respect to the observed background, plotted in Fig. 5.

From our analysis we have to conclude that sterile neutrinos cannot significantly contribute to optical and infrared background. Discarding the hypothesis of sterile neutrinos

⁶ We assumed spectral index of the electron distribution $p=1$, which maximizes the optical and infrared flux.

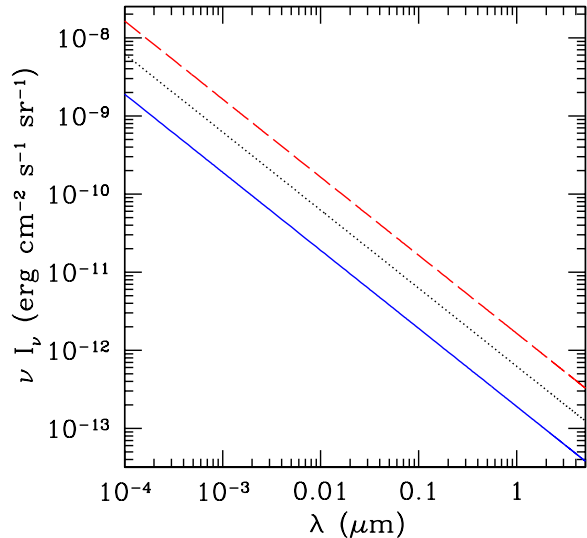


Figure 7. Background due to CMB photons Compton-scattered by electrons produced by sterile neutrinos of masses 215 MeV (*dashed line*), 300 MeV (*dotted*) and 500 MeV (*solid*). Neutrino lifetime is $\tau = 10^{15}$ s; spectral index of electrons $p=1$.

on the basis of our results, the only models which can explain the excess observed in the NIR background are those involving the contribution of Population III stars (Salvaterra & Ferrara 2003; Madau & Silk 2005) and/or of high redshift miniquasars (Madau et al. 2004; Cooray & Yoshida 2004).

4 IMPACT ON REIONIZATION

As briefly discussed in the Introduction, the most recent measurements of the Thomson optical depth (Springel et al. 2003; Kogut et al. 2003; Fan et al. 2003) suggest a complex reionization history, difficult to model without invoking the contribution of "exotic" sources (like very massive Population III stars and miniquasars). Sterile neutrinos have been also proposed as ionization sources, both in the case of radiative decays (Sciama 1982), and, more recently, of pion-decays (HH). In this Section we reexamine this hypothesis, using the calculations presented in Section 2.

4.1 Radiative decay channel

Let us consider first the possible role of radiatively decaying sterile neutrinos. To derive the Thomson optical depth provided by this process, we calculate the hydrogen ionization fraction, x , due to photons emitted by neutrino decays. Under the hypothesis of ionization equilibrium, this can be calculated (Osterbrock 1988) as:

$$(1-x)n_H \int_{E_{th}}^{\infty} 4\pi \frac{dN}{dE dA dt} \sigma_E dE = x^2 n_H^2 \alpha(T), \quad (18)$$

where $n_H = n_{H0} + n_{H+}$ is the total hydrogen number density (n_{H0} and n_{H+} being the neutral and ionized hydrogen number density respectively); $x \equiv n_{H+}/n_H$ is the ionization fraction; $E_{th} = 13.6$ eV, $dN/dE dA dt$ is the photon flux (units

of $\text{cm}^{-2} \text{s}^{-1} \text{sr}^{-1} \text{erg}^{-1}$), $\alpha(T) = 4.18 \times 10^{-13} (T/10^4 \text{K})^{-0.726}$ $\text{cm}^3 \text{s}^{-1}$ is the recombination coefficient; σ_E is the photoionization cross section of hydrogen atoms.

After some calculations reported in Appendix A, in the case of radiatively decaying sterile neutrinos eq. (18) can be expressed as:

$$\frac{x^2(z)}{(1-x(z))} = \frac{n_s(1+z)}{\tau \alpha(T) n_H(0)} \frac{c}{E_0 H_0 [\Omega_{0M}(1+z)^3 + \Omega_\Lambda]^{1/2}} \times \int_{E_{th}/(1+z)}^{E_0/(1+z)} \frac{\sigma_{E(z)} e^{-t(E_0/E_{obs})/\tau} e^{-\tau_{abs}(E_0/E_{obs})}}{\left[\left(\frac{E_0}{E_{obs}} \right)^3 \frac{\Omega_{0M}}{[\Omega_{0M}(1+z)^3 + \Omega_\Lambda]} + \Omega_\Lambda \right]^{1/2}} dE_{obs} \quad (19)$$

where τ_{abs} is defined by eq. (A3).

So far, we have neglected the possibility that the ionizing photon produces a secondary electron which is sufficiently energetic to collisionally ionize additional hydrogen atoms. This is an important effect if $E(z) \gg E_{th}$. To take it into account, we modify the cross section by introducing a factor $[1 + \phi(x(z)) E(z)/E_{th}]$, where (Shull & van Steenberg 1985) $\phi(x) = \mathcal{C} (1-x^a)^b$; for hydrogen ionization $\mathcal{C} = 0.3908$, $a = 0.4092$ and $b = 1.7592$. Adding this term in eq. (19) we finally obtain:

$$\frac{x^2(z)}{(1-x(z))} = \frac{n_s(1+z)}{\tau \alpha(T) n_H(0)} \frac{c}{E_0 H_0 [\Omega_{0M}(1+z)^3 + \Omega_\Lambda]^{1/2}} \times \int_{E_{th}/(1+z)}^{E_0/(1+z)} \frac{e^{-t(E_0/E_{obs})/\tau} e^{-\tau_{abs}(E_0/E_{obs})}}{\left[\left(\frac{E_0}{E_{obs}} \right)^3 \frac{\Omega_{0M}}{[\Omega_{0M}(1+z)^3 + \Omega_\Lambda]} + \Omega_\Lambda \right]^{1/2}} \times \sigma_{E(z)} \left[1 + \phi(x(z)) \frac{E_{obs}(1+z)}{E_{th}} \right] dE_{obs} \quad (20)$$

We solve this equation iteratively, evaluating ϕ and $\tau(E_0/E_{obs})$ at z_{i-1} , where $(z_i - z_{i-1}) \lesssim \epsilon$, with ϵ suitably small (in our calculations $\epsilon = 0.1$ gives a good result).

Finally, we have to include the relic ionization fraction remaining after recombination. At high redshift this fraction can be higher than that due to sterile neutrinos. Therefore, to evaluate $\phi(x)$ and $\tau_{abs}(E_0/E_{obs})$, we take a value $x(z) = \max[x_\nu(z), x_{rel}(z)]$, where $x_\nu(z)$ is the ionization fraction due to sterile neutrino decays and $x_{rel}(z)$ is the residual ionization fraction. For $x_\nu(z)$ we use the value found by solving eq. (20). For $x_{rel}(z)$ we adopt the values derived by Tegmark, Silk, Rees Blanchard, Abel & Palla (1997) from $z=1100$ to $z=20$, and the asymptotic, constant value $x_{rel}(z)=3 \times 10^{-4}$ for $z < 20$. We found that the differences obtained considering other estimates of $x_{rel}(z)$ – as those derived in Jones & Wyse (1985), Seager, Sasselov & Scott (2000), or Shull (2004) – are negligible. The ionized fractions we calculated in this way are shown in Fig. 8. The ionization fraction due to radiatively decaying neutrinos of masses $m_{\nu s} \lesssim 14$ keV (higher masses are prohibited by X-ray measurements) is always $x < 0.1$. For example, the ionization fraction produced by a sterile neutrino of 2 keV (14 keV) exceeds the relic ionization fraction at redshift $z \sim 50$ ($z \sim 200$) and increases up to $x \sim 0.003$ ($x \sim 0.01$) at redshift $z = 10$.

It is then possible to derive the Thomson optical depth τ_e due to radiatively decaying neutrinos using the standard expression

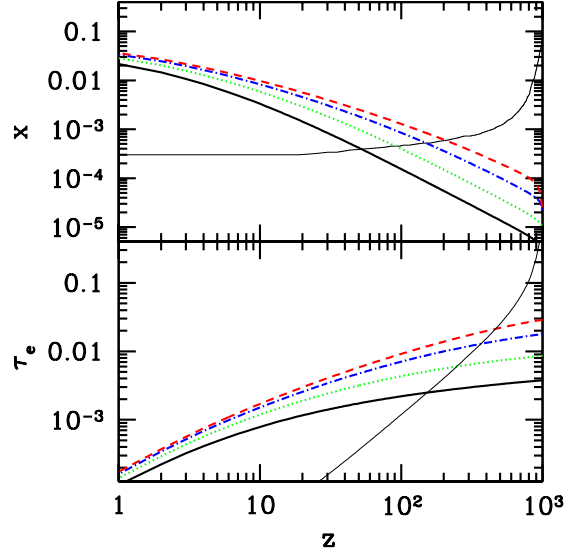


Figure 8. Ionization fraction (*top panel*) and Thomson optical depth (*bottom panel*) due to radiatively decaying neutrinos of masses 2 (*solid line*), 4 (*dotted line*), 8 (*dot-dashed line*) and 14 keV (*dashed line*). The *solid thin line* indicates: in the *top panel* the relic ionization fraction (Tegmark et al. 1997); in the *bottom panel* the Thomson optical depth due to relics.

$$\tau_e = \int_0^z dz \frac{dt}{dz} c \sigma_T n_e(z), \quad (21)$$

where σ_T is the Thomson cross section, $dt/dz = H_0^{-1} [\Omega_{0M}(1+z)^3 + \Omega_\Lambda]^{-1/2}$ and $n_e(z) = n_{H^+}(z) \equiv x(z) n_H(0) (1+z)^3$. The results are shown in Fig. 8. For an integration upper limit $z = 1000$ (i.e. corresponding to the low redshift boundary of the last scattering surface), we find the results reported in Table 1. The contribution of radiatively decaying neutrinos to ionization fraction is negligible, being in the range $3.77 \times 10^{-3} \leq \tau_e \leq 2.86 \times 10^{-2}$ for $m_{\nu s} = 2 - 14$ keV, i.e. much lower than the WMAP best value ($\tau_e = 0.17 \pm 0.04$).

4.2 Pion decay channel

To calculate the ionization fraction due to CMB photons Compton-scattered by electrons produced by heavy sterile neutrinos we use again eq. (18). In this case:

$$\frac{dN}{dE dA dt} = \frac{1}{4\pi} \frac{8\pi^2 r_0^2}{h_P^3 c^2} F(p) (k_B T_0)^{(p+5)/2} E_{obs}^{-(p+1)/2} \times \frac{4.8}{\tau \left[\left(\frac{m_{\nu s}}{m_\pi} \right)^2 - 1 \right]} \frac{3 n_b}{11 \eta} \frac{1}{\int_{\gamma_{min}}^{\gamma_{max}} \gamma^{-p} d\gamma} \frac{c}{H_0} \times \int_z^{z_{decay}} \frac{(1+z) e^{-t(z)} (e^{tC(z)/\tau} - 1)}{[\Omega_{0M}(1+z)^3 + \Omega_\Lambda]^{1/2}} e^{-\tau_{abs}(z, z_{decay})} dz \quad (22)$$

where $\tau_{abs}(z, z_{decay})$ is given by the eq. (A3). Following the same procedure as in previous Section (see also Appendix A), we find:

$$\frac{x^2(z)}{(1-x(z))} = \frac{4\pi}{\alpha(T) n_H(0) (1+z)^2} \int_{E_{th}/(1+z)}^{E_{em}/(1+z)} \frac{dN}{dE dA dt}$$

Table 1. Thomson optical depth due to radiatively decaying and pion-decaying sterile neutrinos (integrated from $z=1000$ to $z=0$).

m_{ν_s} (keV)	τ_e
2	3.77×10^{-3}
4	8.61×10^{-3}
6	1.33×10^{-2}
8	1.78×10^{-2}
10	2.18×10^{-2}
12	2.54×10^{-2}
14	2.86×10^{-2}
m_{ν_s} (MeV)	τ_e
150	5.81×10^{-3}
215	2.14×10^{-3}
250	1.71×10^{-3}
300	1.35×10^{-3}
350	1.13×10^{-3}
400	9.85×10^{-4}
450	8.78×10^{-4}
500	7.96×10^{-4}

$$\times \sigma_{E(z)} \left[1 + \phi(x(z)) \frac{E_{obs}(1+z)}{E_{th}} \right] dE_{obs}, \quad (23)$$

where $dN/dEdAdt$ comes from the eq. (22), $\alpha(T)$, $\sigma_{E(z)}$, E_{th} and $\phi(x(z))$ are the same as defined for radiatively decaying neutrinos. We adopted lifetime $\tau = 10^{15}$ s as suggested by HH. Because of the constraints derived from the HXRB, only masses $215 \lesssim m_{\nu_s} \lesssim 500$ MeV are allowed assuming this lifetime.

The results shown in Fig. 9 imply that the ionization fraction due to pion-decaying neutrinos is negligible at high redshift, being always lower or close to the relic one for $z \gtrsim 30$. At redshifts lower than 20, the contribution of sterile neutrinos becomes more important, albeit $x_e \lesssim 0.1$; as a consequence, the Thomson optical depth (Fig. 9 and Table 1) is very low ($\tau_e < 10^{-2}$). Even for $m_{\nu_s} = 150$ MeV with a lifetime $\tau = 10^{15}$ s (which is however forbidden by HXRB limits), we only obtain $\tau_e = 5.8 \times 10^{-3}$ (Table 1). This result discards pion-decaying neutrinos as a source of reionization, in agreement with the results of Pierpaoli (2004).

4.3 Comparison with previous results

The values of the ionization fraction and of the Thomson optical depth derived in Section 4.2 partially disagree with the scenario drawn by HH, who suggest an early ionization due to pion-decaying neutrinos. In this Section we clarify the possible sources of such discrepancy.

Let us consider first the flux of ionizing photons in the two models. This flux can be derived by integrating eq. (22) from $E_{th}/(1+z)$ to $E_{em}/(1+z)$. At redshift $z = 20$ (the reference redshift in HH) we find that the ionizing photons flux is $\sim 30 \text{ cm}^{-2} \text{ s}^{-1}$. In the case studied by of HH, the flux of ionizing photons can be derived from their equation (10), i.e. $n_b = \epsilon \chi n_e^{prod}$, where n_b is the number density of (re)ionized hydrogen atoms, $\chi = E_e/E_{th}$, n_e^{prod} is the number density of electrons produced by neutrino decays, and $\epsilon \sim 0.3$ is the fraction of the initial energy of the secondary

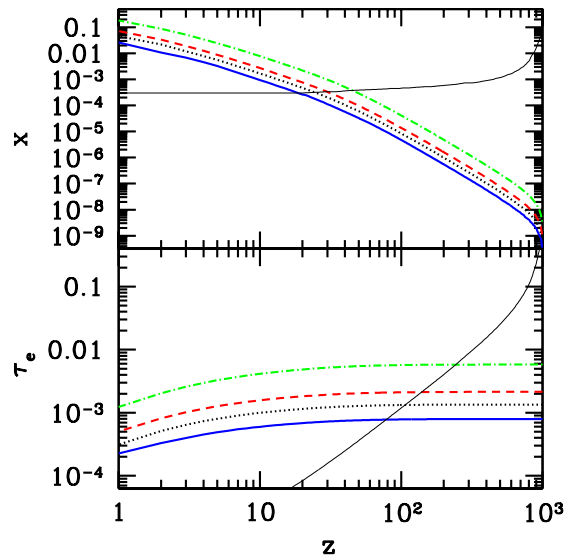


Figure 9. Ionization fraction (*top panel*) and Thomson optical depth (*bottom panel*) due to pion-decaying sterile neutrinos of masses 500 (*solid line*), 300 (*dotted line*), 215 (*dashed line*) and 150 MeV (*dot-dashed line*). The *solid thin line* indicates: in the *top panel* the relic ionization fraction (Tegmark et al. 1997); in the *bottom panel* the Thomson optical depth due to relics.

photoelectrons spent in collisional ionizations (Shull & van Steenberg 1985). In particular, we can write:

$$I = c \epsilon \chi n_e^{prod} \quad (24)$$

At $z = 20$, for $E_e = 100$ MeV, $I \sim 9.7 \times 10^3 \text{ cm}^{-2} \text{ s}^{-1}$, that is a difference of more than 2 orders of magnitude with respect to our result. However, if we take $\epsilon = \chi = 1$, we obtain $I \sim 8.0 \times 10^{-3}$, which is more than 3 orders of magnitude lower than our value. Then, the assumption that an electron of energy E_e is able to produce $\sim \epsilon E_e/E_{th}$ ionizations is crucial, and, we think, quite optimistic. For example, a CMB photon Compton-scattered by such electron at $z \gtrsim 20$ will have an energy much higher than E_{th} , and, because $\sigma_E \propto (E/E_{th})^{-3}$, it is unlikely that this photon immediately interacts with hydrogen atoms. In addition, this high energy photon can be involved in many other processes, like pair production, and its energy does not entirely contribute to reionization.

However, even under the assumption that a primary electron yields χ ionizations, additional physics must be considered. HH (i) do not consider the effect of recombinations, (ii) assume that the density of sterile neutrinos is constant, (iii) neglect the gas clumping factor, (iv) do not weight the photoionization rate by the cross section $\sigma_{E(z)}$. We therefore add these processes to HH's calculation.

The number of recombinations (N_{rec}) and of ionizations (N_{ion}) per unit volume can be written as:

$$\begin{aligned} N_{rec} &= \alpha C x^2 n_b^2 (1+z)^6 \\ N_{ion} &= (1-x) \frac{dn_e}{dt} f_{abs} \epsilon \chi \end{aligned} \quad (25)$$

where $\alpha = 4.18 \times 10^{-13} \text{ cm}^3 \text{ s}^{-1}$ is the recombination coefficient, $C \equiv \langle n_H^2 \rangle / \langle n_H \rangle^2 (\gtrsim 1)$ is the clumping factor, x the ionization fraction and n_b the present baryon density. χ

and ϵ are the same as previously defined. f_{abs} is the fraction of the total radiation which is absorbed at each redshift (to take into account the photoionization cross section). Finally, dn_e/dt is the production rate of primary electrons, i.e. $dn_e/dt = n_e \tau^{-1} (1+z)^3 e^{-t(z)/\tau}$, where $n_e = 4.8 n_a \tau^{-1} ((m_{\nu s}/m_\pi)^2 - 1)^{-1}$ and $n_a = 3/11 n_b \eta^{-1} \text{ cm}^{-3}$ (see Sec. 2.2).

Then, imposing $N_{rec} = N_{ion}$ we find:

$$\frac{x^2}{(1-x)} = \frac{1.31 e^{-t(z)/\tau} f_{abs} \epsilon \chi}{\alpha C n_b \eta (1+z)^3 \tau^2 ((m_{\nu s}/m_\pi)^2 - 1)}, \quad (26)$$

where $t(z)$ is given by eq. (3). For comparison with HH, we adopt $\tau = 10^{15}$ s and $z = 20$. At this redshift, we can neglect⁷ $(1-x)$, because $x \ll 1$. As $E_e = 1/2 (m_{\nu s} - m_\pi)$ and choosing $m_{\nu s} = 215$ MeV (i.e. the minimum mass allowed by the HXRB for $\tau = 10^{15}$ s, corresponding to the maximum x), we obtain:

$$x \sim 0.070 \left(\frac{\epsilon}{0.3} \right)^{1/2} f_{abs}^{1/2} C^{-1/2} \quad (27)$$

Even if $f_{abs} = 1$ and $C = 1$, an ionization fraction $x(z = 20) \sim 0.07 \ll 1$ is found, i.e. incomplete reionization. More realistically, C will be higher than 1, whereas $f_{abs} < 1$. For example, by calculating the difference between the ionizing flux due to Compton scattered CMB photons (see Sec. 4.2) with and without the term $e^{-\tau_{abs}}$ (see eq. (A3)), we find $f_{abs} \sim 0.1$ in the range $500 \geq z \geq 10$. Then, we have $x(m_{\nu s} = 215 \text{ MeV}) \sim 0.022 \left(\frac{\epsilon}{0.3} \right)^{1/2} \left(\frac{f_{abs}}{0.1} \right)^{1/2} C^{-1/2}$. This value is in good agreement with the results of Pierpaoli (2003), but it is a factor 10 higher than that reported in Fig. 9. This difference can be explained with the fact that equation (26) still contains some simplifying assumptions, as the term χ (see previous discussion), instead of a more realistic spectrum for the ionizing radiation.

5 SUMMARY

We have studied the possible contribution of sterile neutrinos decays to the extragalactic X-ray and infrared-optical background, deriving limits on their masses. Such constraints have been then used to assess the impact of ionizing radiation produced by the decays on cosmic reionization. Both radiatively decaying neutrinos and heavy neutrinos decaying into pions and electrons (HH) have been considered.

By calculating the contribution of sterile neutrinos to X-ray background, we have put a strong constraint on the neutrino mass. In particular, by requiring that the estimated flux due to sterile neutrinos does not exceed the SXRb (Moretti et al. 2003; Dijkstra et al. 2004; Bauer et al. 2004), we found that radiatively decaying neutrinos must have masses $m_{\nu s} \lesssim 950$ keV. Much more stringent limits can be found from the comparison with the HXRB. In fact, by requiring that the flux produced by sterile neutrino decays does not exceed the HXRB (Bauer et al. 2004), we find that the mass of radiatively decaying neutrinos must be $m_{\nu s} \lesssim 14$ keV. This constraint on radiatively decaying neutrinos is very important if combined with the results by Viel et al. (2005), who found a lower limit $m_{\nu s} \gtrsim 2$ keV

from the study of power spectrum. Pion-decaying neutrino masses in the range $150 \text{ MeV} \lesssim m_{\nu s} \lesssim 500 \text{ MeV}$ are allowed if the lifetime is longer than 4×10^{17} s. For shorter lifetimes, the minimum mass increases: for example, if $\tau = 10^{15}$ s, $215 \lesssim m_{\nu s} \lesssim 500 \text{ MeV}$.

We have calculated the sterile neutrino decay contribution to the optical and infrared background light. We find that both radiatively and pion-decaying neutrinos give a flux in the optical and NIR range which is several orders of magnitude lower than the observed one. Then alternative sources, as very massive Pop III stars (Salvaterra & Ferrara 2003), must be invoked to explain the detected NIR background excess.

Decaying sterile neutrinos might also be a potential source of cosmological reionization. We derived the ionization fraction and the Thomson optical depth produced by radiatively decaying sterile neutrinos and CMB photons Compton-scattered by electrons produced by heavy (pion-decaying) neutrinos. Radiatively decaying neutrinos produce an optical depth $\tau_e = (0.4 - 3) \times 10^{-2}$, whereas the contribution to reionization of pion-decaying neutrinos is even smaller, yielding an optical depth $\tau_e \approx 10^{-3}$. In conclusion, our calculations suggest that both radiatively- and pion-decaying neutrinos are not viable reionization sources.

ACKNOWLEDGEMENTS

We thank S. Hansen, A. Moretti, P. Tozzi, E. Ripamonti, P. Ullio, T. Schwetz and E. Pierpaoli for useful discussions.

REFERENCES

- Abazajian K., Fuller G. M., Patel M., 2001a, PhRvD, 64b, 3501
- Abazajian K., Fuller G. M., Tucker W. H., 2001b, ApJ, 562, 593
- Abramovitz M., Stegun I. A., 1965, *Handbook of Mathematical Functions*, Dover Publications, Inc, New York
- Astier P. et al. [NOMAD Collaboration], 2001, Phys. Lett. B, 506, 27
- Barkana R., Loeb A., 2001, PhR, 349, 125
- Bauer F. E., Alexander D. M., Brandt W. N., Schneider D. P., Treister E., Hornschemeier A. E., Garmire G. P., 2004, AJ, 128, 2048 [B04]
- Becker R. H., et al., 2001, AJ, 122, 2850
- Bernstein R. A., Freedman W. L., Madore B. F., 2002, ApJ, 571, 56
- Biller S. D. et al., 1998, Phys. Rev. Lett., 80, 2992
- Bode P., Ostriker J. P., Turok, N., 2001, ApJ, 556, 93
- Boehm F., Vogel P., 1987, *Physics of Massive Neutrinos* (Cambridge University Press, New York)
- Bond J. R., Carr B. J., Hogan C. J., 1986, ApJ, 306, 428
- Bowyer S., Korpela E. J., Edelman J., Lampton M., Morales C., Prez-Mercader J., Gmez J. F., Trapero J., 1999, ApJ, 526, 10
- Cen R., 2003, ApJ, 591, 12
- Choudhury T. R., Ferrara A., astro-ph/0411027, accepted for publication in MNRAS
- Colombi S., Dodelson S., Widrow L. M., 1996, ApJ, 458, 1
- Cooray A., Yoshida N., 2004, MNRAS, 351, 71
- Davidson A. F., Kriss G. A., Ferguson H. C., Blair W. P., Bowers C. W., Kimble R. A., 1991, Natur, 351, 128
- De Rjula A., Glashow S. L., 1980, Phys. Rev. Lett., 45, 942
- Dijkstra M., Haiman Z., Loeb A., 2004, ApJ, 613, 646 [D04]
- Dolgov A. D., 2002, Phys.Rept., 370, 333 (hep-ph/0202122)

⁷ This results in a difference of the order of 10^{-4}

- Dolgov A. D., Fukugita M., 1992, Phys. Rev. D 46, 5378
- Dolgov A. D., Hansen S. H., 2002, APH, 16, 339
- Drees M., Wright D., 2000, hep-ph/0006274
- Fan X., et al., 2003, AJ, 125, 1649
- Furlanetto S., Loeb A., 2004, in press at ApJ, astro-ph/0409656
- Gruber D. E., 1992, in *The X-Ray Background*, ed. X. Barcons & A. C. Fabian (Cambridge: Cambridge Univ. Press), 44
- Haiman Z., Holder G. P., 2003, ApJ, 595, 1
- Hansen S. H., Haiman Z., 2004, ApJ, 600, 26
- Hansen S. H., Lesgourgues J., Pastor S., Silk J., 2002, MNRAS, 333, 544
- Hauser M. G., Dwek E., 2001, ARA&A, 39, 249
- Henry R. C., Feldman P. D., 1981, Phys. Rev. Lett., 47, 618
- Holberg J. B., Barger H. B., 1985, ApJ, 292, 16
- Hornscheimer A. E. et al., 2001, ApJ, 554, 742
- Jones B. J. T., Wyse R. F. G., 1985, A&A, 149, 144
- Kelsall T., Weiland J. L., Franz B. A., Reach W. T., Arendt R. G., et al., 1998, ApJ, 508, 44
- Kimble R., Bowyer S., Jakobsen P., 1981, Phys. Rev. Lett., 46, 80
- Kogut A., et al., 2003, ApJS, 148, 161
- Madau P., Pozzetti L., 2000, MNRAS, 312, L9
- Madau P., Rees M. J., Volonteri M., Haardt F., Oh S. P., 2004, ApJ, 604, 484
- Madau P., Silk J., 2005, MNRAS, 359L, 37
- Magliocchetti M., Salvaterra R., Ferrara A., 2003, MNRAS, 342, 25
- Matsumoto T., Cohen M., Freund M. M., Kawaka M., Lim M., et al., 2000, in *ISO Surveys of a Dusty Universe*. Lecture Notes in Physics vol. 548, ed. Lemke D., Stickel M., Wilke K., pp.96-105, Berlin Heidelberg: Springer Verlag
- Massó E., Toldrà R., 1999, Phys. Rev. D, 60, 083503
- Moretti A., Lazzati D., Campana S., Tagliaferri G., 2002, ApJ, 570, 502
- Moretti A., Campana S., Lazzati D., Tagliaferri G., 2003, ApJ, 588, 696 [M03]
- Narayanan V. K., Spergel D. N., Dav R., Ma C. P., 2000, ApJL, 543, 103
- Osterbrock D. E., *Astrophysics of Gaseous Nebulae and Active Galactic Nuclei*, Univ. Science Books, 1988
- Ostriker J. P., Steinhardt, P., 2003, Sci, 300, 1909
- Padmanabhan T., *Structure Formation in the Universe*, Cambridge University Press, 1995
- Pierpaoli E., 2004, Phys. Rev. Lett., 92, 031301
- Rephaeli Y., Szalay A. S., 1981, Phys. Lett. B, 106, 73
- Ressel M. T., Turner M. S., 1990, Comments Astrophys., 14, 323
- Rybicki G. B., Lightman A. P., *Radiative Processes in Astrophysics*, San Francisco, 1979
- Salvaterra R., Ferrara A., 2003, MNRAS, 339, 973
- Santos M. R. Bromm V., Kamionkowski M., 2002, MNRAS, 336, 1082
- Schaerer D., 2002, A&A, 382, 28
- Sciama D. W., 1982, MNRAS, 198, 1
- Sciama D. W., 1990, ApJ, 364, 549
- Sciama D. W., 1993, Cambridge lecture notes in physics, 3, Cambridge Univ. Press
- Seager S., Sasselov D. D., Scott D., 2000, ApJS, 128, 407
- Shipman H. L., Cowsik R., 1981, ApJL, 247, 111
- Shull J. M., van Steenberg M. E., 1985, ApJ, 298, 268
- Shull J. M., 2004, to appear in *Astrophysics in the Far Ultraviolet* (FUSE 5th Year Conf), astro-ph/0410189
- Soltan, A. M. 2003, A&A, 408, 39
- Sommer-Larsen J., Dolgov A., 2001, ApJ, 551, 608
- Spergel, D. N., et al., 2003, ApJS, 148, 175
- Stecker F. W., 1980, Phys. Rev. Lett., 45, 1460
- Tegmark M., Silk J., Rees M. J., Blanchard A., Abel T., Palla F., 1997, ApJ, 474, 1
- Tozzi P. et al., 2001, ApJ, 562, 42
- Viel M., Lesgourgues J., Haehnelt M. G., Matarrese S., Riotto A., 2005, PhRvD, 71, 3534
- Wright E. L., 1997, American Astronomical Society, 191st AAS Meeting, Bulletin of the American Astronomical Society, Vol. 29, p.1354
- Wright E. L., 1998, ApJ, 496, 1
- Wright E. L., Reese E. D., 2000, ApJ, 545, 43
- Wright E. L., 2001, ApJ, 553, 538
- Wu X., Xue Y., 2001, ApJ, 560, 544

APPENDIX A: IONIZATION FRACTION BY RADIATIVELY DECAYING STERILE NEUTRINOS

The hydrogen ionization fraction, x , due to photons emitted by neutrino decays can be derived, under the hypothesis of ionization equilibrium (Osterbrock 1988), as:

$$(1-x)n_H \int_{E_{th}}^{\infty} 4\pi \frac{dN}{dE dA dt} \sigma_E dE = x^2 n_H^2 \alpha(T), \quad (\text{A1})$$

where $n_H = n_{H0} + n_{H+}$ is the total hydrogen number density (n_{H0} and n_{H+} being the neutral and ionized hydrogen number density respectively); $x \equiv n_{H+}/n_H$ is the ionization fraction; $E_{th} = 13.6$ eV, $dN/dE dA dt$ is the photon flux (units of $\text{cm}^{-2} \text{s}^{-1} \text{sr}^{-1} \text{erg}^{-1}$), $\alpha(T) = 4.18 \times 10^{-13} (T/10^4 \text{K})^{-0.726} \text{cm}^3 \text{s}^{-1}$ is the recombination coefficient; σ_E is the photo-ionization cross section of hydrogen atoms.

We have derived $dN/dE dA dt$ from eq. (2). The specific flux will be:

$$\frac{dN}{dE dA dt} = \frac{1}{4\pi} \frac{c}{H(z)} \frac{n_s(z)}{\tau} \int_0^{z'} e^{-t(z')/\tau} e^{-\tau_{abs}(z')} \frac{\delta((1+z')E(z) - E_0)}{(1+z') [(1+z')^3 \Omega_M(z) + \Omega_\Lambda]^{1/2}} dz', \quad (\text{A2})$$

where, in the reference frame of the hydrogen atom, z' and 0 are respectively the redshift at which the sterile neutrino decays emitting a photon and the redshift at which this photon ionizes the hydrogen atom. Passing from the reference frame of the hydrogen atom to the reference frame of an observer (at redshift 0), the redshifts z' and 0 respectively correspond to z_{em} and z , through the relation $(1+z') = (1+z_{em})/(1+z)$. As in Section 2, E_0 is the energy of the photon when it was emitted. $\tau_{abs}(z')$ takes into account the fact that a photon emitted by a sterile neutrino will be absorbed, due to hydrogen photo-ionization, after a certain mean free path λ_H . It is given by:

$$\tau_{abs}(z') \equiv \int_0^{z'} \lambda_H^{-1}(\tilde{z}) \frac{dl}{d\tilde{z}} d\tilde{z} \quad (\text{A3})$$

where dl is the proper distance element. The mean free path of the photon, λ_H , can be expressed as:

$$\lambda_H(z) \equiv \frac{1}{n_{H0}(z) \sigma_{E(z)}} = \frac{1}{n_{H0}(0) (1+z)^3 (1-x(z)) \sigma_{E(z)}}.$$

Because $n_s(z) = n_s(1+z)^3$ and taking into account that $\delta((1+z')E(z) - E_0) \neq 0$ if and only if $(1+z') = E_0/E(z)$, eq. (A2) becomes

$$\frac{dN}{dE dA dt} = \frac{1}{4\pi} \frac{c}{H(z)} \frac{n_s(1+z)^3}{\tau} e^{-t(z')/\tau} e^{-\tau_{abs}(z')} \frac{1}{E_0 \left[\left(\frac{E_0}{E(z)} \right)^3 \Omega_M(z) + \Omega_\Lambda \right]^{1/2}} \quad (\text{A4})$$

Substituting $E(z) = E_{obs}(1+z)$ (E_{obs} being the energy of the photon today), $H(z) = H_0 [\Omega_{0M}(1+z)^3 + \Omega_\Lambda]^{1/2}$ and $\Omega_M(z) = \frac{\Omega_{0M}(1+z)^3}{[\Omega_{0M}(1+z)^3 + \Omega_\Lambda]}$, we obtain

$$\frac{dN}{dE dA dt} = \frac{1}{4\pi} \frac{c}{H_0 [\Omega_{0M}(1+z)^3 + \Omega_\Lambda]^{1/2}} \frac{n_s(1+z)^3 e^{-t(z')/\tau} e^{-\tau_{abs}(z')}}{\tau E_0 \left[\left(\frac{E_0}{E_{obs}} \right)^3 \frac{\Omega_{0M}}{[\Omega_{0M}(1+z)^3 + \Omega_\Lambda]} + \Omega_\Lambda \right]^{1/2}}, \quad (\text{A5})$$

where, assuming that $\Omega_\Lambda \ll (1+z')^3 \Omega_M(z)$, $\Omega_\Lambda < (1+z)^3 \Omega_{0M}$ and $\Omega_M(z) \sim 1$, and substituting $(1+z') = (1+z_{em})/(1+z)$ and $(1+z_{em}) = (E_0/E_{obs})$, we can find

$$t(z') \simeq \frac{2}{3} H_0^{-1} \Omega_{0M}^{-1/2} (E_0/E_{obs})^{-3/2} = t(E_0/E_{obs}) \quad (\text{A6})$$

Similarly, we can also show that

$$\tau_{abs}(z') = \int_0^{z'} \lambda_H^{-1}(\tilde{z}) \frac{dl}{d\tilde{z}} d\tilde{z} = \int_z^{z_{em}} \lambda_H^{-1}(\tilde{z}) \frac{dl}{d\tilde{z}} d\tilde{z} = \tau_{abs}(E_0/E_{obs}) \quad (\text{A7})$$

Finally we can write

$$\int_{E_{th}}^{\infty} 4\pi \frac{dN}{dE dA dt} \sigma_E dE = \frac{c}{H_0} \int_{E_{th}}^{E_0} \frac{n_s(1+z)^3}{\tau [\Omega_{0M}(1+z)^3 + \Omega_\Lambda]^{1/2}} \frac{\sigma_{E(z)} e^{-t(E_0/E_{obs})/\tau} e^{-\tau_{abs}(E_0/E_{obs})}}{E_0 \left[\left(\frac{E_0}{E_{obs}} \right)^3 \frac{\Omega_{0M}}{[\Omega_{0M}(1+z)^3 + \Omega_\Lambda]} + \Omega_\Lambda \right]^{1/2}} dE(z) \quad (\text{A8})$$

where the upper limit of integration, E_0 , takes into account that the photon energy at redshift z cannot be larger than at redshift z_{em} , when it was emitted. We can make a change of integration variable ($E(z) = (1+z)E_{obs}$), obtaining:

$$\int_{E_{th}}^{\infty} 4\pi \frac{dN}{dE dA dt} \sigma_E dE = \frac{c}{H_0} \int_{E_{th}/(1+z)}^{E_0/(1+z)} \frac{n_s(1+z)^4}{\tau [\Omega_{0M}(1+z)^3 + \Omega_\Lambda]^{1/2}} \frac{\sigma_{E(z)} e^{-t(E_0/E_{obs})/\tau} e^{-\tau_{abs}(E_0/E_{obs})}}{E_0 \left[\left(\frac{E_0}{E_{obs}} \right)^3 \frac{\Omega_{0M}}{[\Omega_{0M}(1+z)^3 + \Omega_\Lambda]} + \Omega_\Lambda \right]^{1/2}} dE_{obs} \quad (\text{A9})$$

For $\sigma_{E(z)}$ we used the following approximation (Osterbrock 1988):

$$\sigma_{E(z)} = \sigma_{th} \left[\beta \left(\frac{E_{obs}(1+z)}{E_{th}} \right)^{-s} + (1-\beta) \left(\frac{E_{obs}(1+z)}{E_{th}} \right)^{-(s+1)} \right], \quad (\text{A10})$$

where $\sigma_{th} = 6.30 \times 10^{-18} \text{ cm}^2$, $\beta=1.34$ and $s=2.99$.

Finally, substituting eq. (A9) into eq. (A1), reordering, and substituting $n_H(z) = n_H(0)(1+z)^3$, we obtain the expression for the ionization fraction:

$$\frac{x^2(z)}{(1-x(z))} = \frac{n_s(1+z)}{\tau \alpha(T) n_H(0)} \frac{c}{E_0 H_0 [\Omega_{0M}(1+z)^3 + \Omega_\Lambda]^{1/2}} \int_{E_{th}/(1+z)}^{E_0/(1+z)} \frac{\sigma_{E(z)} e^{-t(E_0/E_{obs})/\tau} e^{-\tau_{abs}(E_0/E_{obs})}}{\left[\left(\frac{E_0}{E_{obs}} \right)^3 \frac{\Omega_{0M}}{[\Omega_{0M}(1+z)^3 + \Omega_\Lambda]} + \Omega_\Lambda \right]^{1/2}} dE_{obs} \quad (\text{A11})$$